sustainability

MDPI

Article

Investigating Asphalt Self-Healing with Colorless Binder and Pigmented Rejuvenator

Tiago Ribeiro [1], Ana Cristina Freire [2], Margarida Sá-da-Costa [2], João Canejo [3], Vinicius Cordeiro [1] and Rui Micaelo [4,*]

[1] Department of Civil Engineering, School of Science and Technology, Universidade NOVA de Lisboa, 2829-516 Caparica, Portugal
[2] National Laboratory for Civil Engineering, 1700-111 Lisbon, Portugal
[3] CENIMAT | i3N, Department of Materials Science, School of Science and Technology, NOVA University Lisbon and CEMOP/UNINOVA, 2829-516 Caparica, Portugal
[4] CERIS, Department of Civil Engineering, School of Science and Technology, Universidade NOVA de Lisboa, 2829-516 Caparica, Portugal
* Correspondence: ruilbm@fct.unl.pt

Abstract: Despite asphalt self-healing with encapsulated rejuvenators having been intensively researched over the last decade, there is still uncertainty about the performance advantages granted by this technology. As a way of adding to the existing set of research methodologies, this study aimed to test the feasibility of a visual method to investigate the working mechanism of encapsulated rejuvenators in the bituminous mixture. For this purpose, clear bituminous mixtures were produced using a colorless synthetic binder and a pigment was added to the rejuvenator incorporated in the calcium alginate capsules. The internal structure of the bituminous mixtures containing these capsules was inspected both on loaded and unloaded specimens. The colored rejuvenator was also directly added to cracked specimens and its distribution was studied, along with the interaction between the rejuvenator and the synthetic binder. The results show that the rejuvenator could modify the binder to a limited extent, and the bituminous mixtures containing capsules showed evidence of rejuvenator release. It is demonstrated that the aggregate gradation of mixtures has a significant effect on capsule damage and rejuvenator release. However, the pigment can be filtrated from the rejuvenator by the capsule polymer structure and the asphalt. Even though the methodology presented some constraints, it has been proven to be capable of achieving the initial goal, while also acting as an important first step in the visual study of rejuvenator release in asphalt.

Keywords: self-healing materials; bituminous materials; rejuvenator; encapsulation; experimental methods

Citation: Ribeiro, T.; Freire, A.C.; Sá-da-Costa, M.; Canejo, J.; Cordeiro, V.; Micaelo, R. Investigating Asphalt Self-Healing with Colorless Binder and Pigmented Rejuvenator. *Sustainability* **2023**, *15*, 4556. https://doi.org/10.3390/su15054556

Academic Editor: Antonio D'Andrea

Received: 30 January 2023
Revised: 26 February 2023
Accepted: 1 March 2023
Published: 3 March 2023

1. Introduction

Transportation is a vital aspect of any society, and improvements in travel speed and capacity have had significant positive economic and social impacts. However, since the current practices are resource-intensive, the maintenance of these infrastructures can be costly and have a high environmental impact, especially when the applied materials are not re-used [1]. Hence, the road agencies' budget allocated to maintenance is often insufficient (e.g., in the USA, the estimated deficit is USD 92 billion [2]), and even with an adequate planning of maintenance works, the performance of current materials limits the required reduction in budgetary needs [3]. In addition, most countries have agreed on ambitious climate goals, such as the European Green Deal [4], which aims to reach by 2050 the neutrality in greenhouse gas emissions of a "fair and prosperous society, with a modern, resource-efficient and competitive economy".

Currently, most roads are constructed with flexible pavements made of bituminous materials, which are designed to achieve a service life of 10 to 30 years, but require repaving

every 8 to 15 years [5] due to the hardening of bitumen over time [6], which can increase the likelihood of surface cracking [7]. This occurs because bitumen is an organic substance that is affected by oxygen, ultraviolet radiation, and temperature changes. Various methods, such as recycling and resurfacing with rejuvenating oils, have been used to repair and restore pavement properties, but they impose road traffic restrictions and/or closures and have some environmental impacts [8]. However promising the heating methods, which reduce the viscosity of bitumen and facilitate self-healing [9], may be, they require large amounts of energy.

This study explores a passive method, such as the one of encapsulating rejuvenating oils within bituminous mixture. This can be a way to improve the endogenous self-healing capabilities of bitumen and to extend the service lives of roads without requiring road closures and with less environmental impact, specifically regarding the consumption of energy and raw materials. This technique takes advantage of the asphalt's ability to self-heal, which was first reported in 1967 [10]. Various mechanisms have been proposed to explain this phenomenon at different scales [11]. Processes such as molecular interdiffusion and capillary flow have been reported to contribute to asphalt self-healing [12]. In a broad sense, these processes are dependent on the binder viscosity and its free surface energy. The asphalt self-healing process can be divided into three key phases: flow, wetting, and interdiffusion [12]. Flow describes the phase during which the sides of a crack come together. This leads to the next step, wetting, which occurs when the surfaces are close enough to start interacting, and hence form an interface. Molecular interdiffusion between the two sides finally leads to the recovery of the properties of the material.

Capsules containing rejuvenators or "softening agents" [13] are intended to expedite the aforementioned flow deformation phase, since asphalt self-healing requires significant rest periods to occur, which is incompatible with regular traffic patterns [14]. The aim of encapsulating rejuvenating oils within the bituminous mixture is to extend the self-healing capabilities of bitumen and improve its durability, ultimately leading to less maintenance and repaving actions being required during the infrastructure life cycle, and to achieving more sustainable transport infrastructures.

While the working mechanism of encapsulated rejuvenators is theoretically sound, the performance benefits of their additional inclusion in a bituminous mixture are still unclear. Specifically, in the case of calcium alginate capsules containing vegetable oil, a type of encapsulated rejuvenator, previous studies have had varying results. Following the addition of these capsules to a mixture, drastic increases in self-healing ability have been reported, but at the expense of the mixture stiffness modulus and fatigue life [15]. Others have shown that these capsules can provide mild increases in fatigue resistance or self-healing, often with one coming at the expense of the other, while somewhat sacrificing resistance to plastic deformation [16]. These different findings highlight the need to further study the behavior of these encapsulated rejuvenators, particularly calcium alginate capsules.

One of the key ways to develop an understanding of the working mechanism behind this technology is to study the rejuvenator dispersion and its interaction with the binder. To do so, three modern experimental techniques have been used: infrared spectroscopy, fluorescence microscopy, and computed tomography scans.

Infrared spectroscopy is a technique that measures the interaction between infrared radiation and the chemical bonds of the compounds being studied. Parameters like emission or absorption can be measured and their results can be plotted as a function of the wavelength. This makes it possible to determine, for example, the rejuvenator content in a bitumen sample [17]. This technique, while offering great insights into the compositional changes in a sample, also poses some challenges when applied to the study of encapsulated rejuvenators in asphalt. These challenges mainly stem from the fact that it can be difficult to extract samples from the bituminous mixture specimen, which are representative of different areas around capsules and/or damaged areas [18].

Fluorescence microscopes work by irradiating a sample with the required wavelength radiation (typically ultraviolet light), and by separating the fainter, longer-wavelength light emitted by it from the excitation light [12]. By coupling this phenomenon with the great visual detail enabled by a microscope, very small details in a sample can be tracked, which would otherwise be invisible to the naked eye (due to their size or to not standing out in the visible light range). This technique can be used to detect substances incorporated in the bitumen (e.g., polymer modifiers), which are not visible in its dark mass, but its effectiveness is diminished when the contrast between the various constituents in a sample decreases. When applied to bituminous mixtures containing encapsulated rejuvenators, fluorescent microscopy results in more complex images in which the aggregate, capsule and rejuvenator may be hard to distinguish. Thus, this technique has been mostly applied to samples of bitumen containing encapsulated rejuvenators [7].

Computed tomography (CT) scans use an X-ray source to produce slices of the sample internal structure, in which the different constituents are identified by different grayscale values. These slices are then combined to form a complete scan of the specimen. While very insightful, this technique also has its limitations. Firstly, the pixel and the voxel dimensions (resolution) of images can vary widely (1.25–100 µm) depending on the definitions and equipment used [16,19]. This means that, when an asphalt sample is analyzed at two different points in time, small microstructural differences, such as microcracks, can be hard to detect. Studying a three-dimensional rendering of a crack instead of slices can attenuate this problem, yet it does not change the fact that the small samples can be exposed to changes in temperature inside the scanner, which might alter the mixture's internal structure to some degree. Secondly, despite the pixel grayscale value varying with the density of the material, it is very difficult to distinguish between mastic volumes with different rejuvenator contents because bitumen and rejuvenator have similar densities. Finally, CT scanners are not largely available in many research institutions.

In summary, innovative solutions are needed to steer the digital and green transitions planned in transport infrastructures. Asphalt self-healing with encapsulated rejuvenator is one hypothesis employed to address these objectives by improving long-term durability and resilience with minimum maintenance needs [20]. Previous investigations have demonstrated the concept of using capsules to improve asphalt's self-healing capacity; however, the conclusions obtained from performance testing did not always conform to subsequent studies. Hence, it is considered that this asphalt system, composed of various-size aggregates, bitumen and capsules, is very complex, and therefore new experimental approaches are still needed to fully understand it and to advance its maturity.

2. Objectives and Scope

The objective of this study was to investigate the viability of an innovative method of studying rejuvenator release, by producing bituminous mixtures with added encapsulated rejuvenator, in which both the rejuvenator and the capsules can be easily seen and studied. This was accomplished by producing mixtures with a colorless (clear or light-colored) binder and by coloring the rejuvenating agent with an adequate pigment.

The experimental plan that supports the investigation was developed to address four key issues: (i) rejuvenator pigmentation and production of pigmented capsules; (ii) rejuvenator–colorless binder interaction; (iii) microstructure of the bituminous mixture with colorless binder and bitumen; and (iv) dispersion of pigmented rejuvenator in the bituminous mixture.

For the first issue, the effect of different pigments on the natural binder color was initially analyzed, and after selecting the pigments, the capsules containing the pigmented rejuvenator were produced by the ionotropic gelation method. Following previous studies [21,22], the rejuvenator selected in this study was sunflower seed oil. The pigmented capsules were characterized in terms of size and mechanical strength.

The rejuvenator–colorless binder interaction was evaluated on the basis of the rheological behavior of the binder with varying rejuvenator contents, with the solubility of the binder in the rejuvenator at an intermediate service temperature.

To investigate the microstructure of the bituminous mixture with colorless binder and bitumen, cylindrical specimens with and without pigmented capsules were produced and their internal structure was analyzed. Then, to study the dispersion of pigmented oil in the bituminous mixture, the asphalt specimens were loaded to induce damage. In specimens without capsules, pigmented oil was injected into cracks.

3. Materials and Methods

3.1. Colorless Binder

A synthetic (colorless) binder Recofal S100-P, supplied by Repsol, was used in this study. This product is a clear, light-colored binder, with physical and rheological properties designed to resemble conventional bitumen (see Table 1). The binder is supplied in pellets (see Figure 1g) and is especially suited to applications where pigmentation is required.

Table 1. Synthetic binder characteristics (product data sheet information).

Characteristics	Method	Unit	Specification
Density	EN 15326	g/cm^3	0.95–1.15
Penetration at 25 °C	EN 1426	0.1 mm	20–50
Softening point	EN 1427	°C	≥85
Resistance to hardening	EN 12607-1		
Retained penetration		%	≥80
Softening point increase		°C	≤10
Change in mass		%	≤1.5
Brookfield viscosity at 160 °C	EN 13303	cP	≥400
Fraass breaking point	EN 12593	°C	≤−20

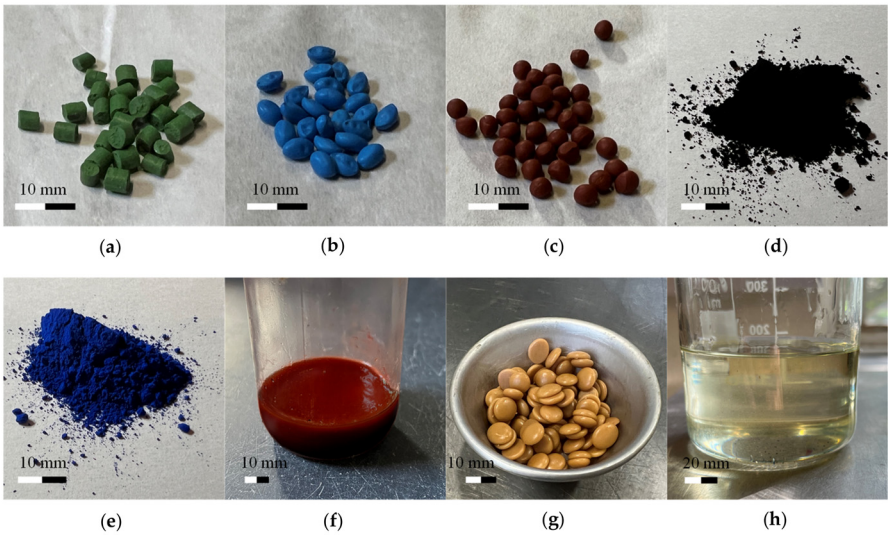

Figure 1. Materials. (**a**–**c**) Pellet pigments (green, blue, and red); (**d**–**e**) powder pigments (black and blue); (**f**) red liquid pigment; (**g**) synthetic binder; (**h**) sunflower seed oil.

3.2. Pigments

Different types of pigments were tested in this study (see Figure 1a–f). Three pigments supplied in pellets were used, which comprised a mixture of inorganic pigment and polymer (blue and green Colorfalt, by Ventraco, and red Ravasol COLOR+ R from Ravago Chemicals). Two powder inorganic pigments were used, carbon black (PBk7) and primary blue (PB15). Finally, red fat-soluble food coloring liquid pigment (sunflower oil based) from Decora was also used.

3.3. Calcium Alginate Capsules

To produce the pigmented rejuvenator, the pigment was added dropwise to the rejuvenator under a magnetic stirrer until reaching the defined content or the maximum content that could be incorporated. For the pigments in pellets, the rejuvenator was preheated to 150 °C to soften the polymer structure and enable the pigment dispersion in the rejuvenator. The red fat-soluble food coloring liquid pigment was mixed with the rejuvenator in equal proportions by weight.

The capsules used in this study contained sunflower seed oil (Figure 1h) as the rejuvenating agent [5]. Sodium alginate from Sigma-Aldrich and calcium chloride from Alfa Aesar were also used. The capsules were produced by the following procedure: (1) the pigmented sunflower seed oil was mixed with water until the oil was evenly dispersed; (2) sodium alginate was added to the mixture while it was stirred at a high rate of speed, producing an emulsion, with continuous agitation for 15 min; (3) a 2% aqueous solution of calcium chloride was prepared; (4) the oil, water, and alginate emulsion was poured into a dropping funnel, which was then placed over the calcium chloride solution (with a 2 cm separation between the nozzle and the solution), while the latter was slowly stirred by a magnetic stirrer; (5) the funnel's tap was regulated to enable the steady dropping of the emulsion in small beads; (6) the newly formed calcium alginate capsules were kept in the calcium chloride bath for an additional fifteen minutes after the last drop, to ensure the thorough polymerization of all capsules; (7) the capsules were then removed from the calcium chloride solution and washed with ethanol, to limit the quantity of oil on their surface. The capsules were dried at ambient temperature and stored in a freezer inside plastic bags.

The capsules were produced with the oil modified with both red pigments (A—pellets and B—fat-soluble food coloring liquid pigment). Capsules A-1 and B were produced using an oil-to-water ratio (O/W) (v/v) of 0.1 and an oil-to-alginate ratio (O/Alg) of 3 mL/g. In addition, capsules A-2 were produced with an oil-to-water ratio (O/W) (v/v) of 0.2 and an oil-to-alginate ratio (O/Alg) of 6 mL/g.

To determine the size of capsules, these were photographed from top and side views and then inspected with *ImageJ* software package. The average dimension was calculated from three line measurements taken on the capsule (2 orthogonal measures on top view and 1 side measure for the thickness).

The mechanical strength of the capsules was determined under uniaxial compression (1 mm/minute) at room temperature. To evaluate the effect of high temperature during asphalt production, a batch of capsules was heated to 150 °C for 10 min and then let to cool to room temperature before loading.

3.4. Asphalt Specimen Preparation

Two types of bituminous mixtures were studied: continuously graded asphalt concrete (AC 14 surf/bin/reg) and discontinuous stone mastic asphalt (SMA 11). Limestone aggregate fractions of 12/20 mm, 4/12 mm and 0/4 mm were used, as well as filler (limestone powder). The binders used consisted of bitumen 35/50 and colorless binder. Regarding both mixture types with the colorless binder, three different contents (w/w of the final mixture) of capsules (0%; 1.25%; 2.00%) were used. Table 2 summarizes the asphalt design composition (w/w) used in the study.

Both cylindrical and prismatic specimens were fabricated with the two mixture types. To produce Marshall-type cylindrical test specimens (with a diameter of 101.6 mm and a height of approximately 63.5 mm), the aggregate mixes were weighed out and placed in a laboratory oven at 175 °C for three hours, along with all the necessary tools and moulds. In a separate oven, the binder was heated to 150 °C for the same period. For each specimen, its constituent aggregates were placed into a mixing bowl, after which the required amount of binder was poured in. The bowl was then attached to a Hobart asphalt stand mixer, and the mixing process was initiated. This process took a total of four minutes, during which the mixer's gas burner was carefully controlled to keep temperatures in the range of 140 °C

to 160 °C. If capsules were to be added, this would be done at the third minute. After mixing, the mixtures were placed into Marshall moulds and compacted using a Marshall compactor. For the asphalt concrete mix, 75 blows were used on each side, while 50 were used for the stone mastic asphalt.

Table 2. Asphalt design composition (*w*/*w*).

Constituents	AC 14	SMA 11
Aggregates	95.0%	94.7%
12/20 mm	(23%)	-
4/12 mm	(28.0%)	(70.0%)
0/4 mm	(46.0%)	(23.0%)
filler	(3.0%)	(7.0%)
Binder	5.0%	5.3%
Capsules *	0%, 1.25%, 2.00%	0%, 1.25%, 2.00%

* *w*/*w* ratio of final mixture.

To fabricate the prismatic specimens (10.0 × 30.5 × 5.0 cm), the bituminous mixtures were produced with a similar procedure and were roller-compacted in slabs (30.5 × 30.5 × 5.0 cm). Roller compaction was controlled by the specimen height. The slab was sawn into beams. Prismatic specimens were fabricated only without capsules.

3.5. Rheological Behavior of Colorless Binder

Dynamic shear rheometer (DSR) testing was performed on the colorless binder modified with different contents of sunflower seed oil (*w*/*w*): 0%, 2.5%, 5%, and 10%. The oil was mixed with the binder at 150 °C and then poured into disk-shaped silicon moulds (with diameters of 8 mm and 25 mm).

The linear viscoelastic rheological behavior of binders was characterized with a frequency sweep test (FS) (0.1 to 100 rad/s) under strain-controlled mode at 20 °C and 60 °C. To determine an appropriate strain amplitude to be used in the FS tests, a set of four Linear Viscoelastic Region (LVR) tests was conducted, in which the samples used contained 0% and 10% oil at 20 °C and 60 °C. A strain amplitude of 0.01% was found to be in the linear region for these materials.

3.6. Colorless Binder Solubility in Rejuvenator at Room Temperature

The solubility in the sunflower seed oil (rejuvenator) of the colorless binder and of the bitumen at room temperature was compared based on an experiment derived from the procedure used to determine the affinity between aggregate and bitumen (EN 12697-11:2020). The following steps were followed:

- Two mixtures were produced, one using bitumen 35/50 and the other a colorless binder;
- After mixing, the mixtures were let to cool on trays, which were lightly coated with silicone compound;
- The mixtures were placed over a perforated plastic film that was then lightly wrapped around the aggregates;
- The bundles were weighed and put into beakers, which were then filled with approximately 170 g of sunflower seed oil each;
- The aggregate bundles were weighed and photographed at one-hour intervals for six hours, and at 24, 25, and 48 h. Each time, the oil was allowed to drain for two minutes before weighing the bundle.

For the mixtures, 150 g of aggregate between 8 mm and 11.2 mm were mixed with 16 g of binder. The binders were heated to their respective mixing temperatures, and the aggregate was heated to 175 °C. In a mixing bowl over a heating mantle, the aggregates were mixed by hand with the binder, ensuring that these were thoroughly covered.

3.7. Mechanical Testing of Asphalt Specimens

The mechanical testing of asphalt specimens was intended to induce damage in specimens to enable the investigation of the mechanisms preceding asphalt self-healing, i.e., rejuvenator release from capsules and rejuvenator dispersion in asphalt. Based on previous studies [15,16] on calcium alginate capsules, the encapsulated agent was entrapped in a 3D continuous porous polymer structure and its release required a combination of structural cracking and compression loads.

Hence, the cylindrical specimens containing encapsulated rejuvenators were subjected to confined uniaxial compression to ensure both the capsule damage and the compression required to release the oil (see Figure 2a). A load of 200 kN was applied on the top surface of the specimen placed in the compaction steel mould, which resulted in a final vertical deformation of 2–6 mm depending on the mixture type and capsule content. After loading, the specimens remained in the mould for 1 day at room temperature, thus enabling the released oil to distribute throughout cracks and diffuse into the mastic. Then, the specimens were broken with a chisel and hammer to inspect the capsule and the oil distribution in the specimen.

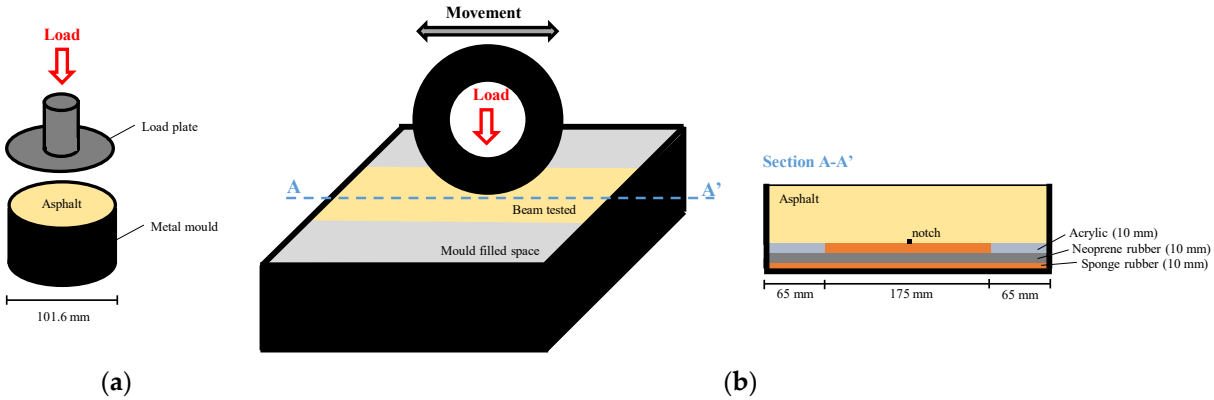

Figure 2. Mechanical testing configuration: (**a**) confined uniaxial compression; (**b**) cyclic bending.

The prismatic specimens of bituminous mixtures without encapsulated rejuvenators were subjected to cyclic bending loading using a wheel tracking simulator without heating (27 °C, average temperature registered in the equipment chamber). This test was intended to realistically simulate fatigue damage on asphalt specimens, which were then used to study the pigmented oil percolation through cracks and diffusion in the mastic. Thus, to ensure bottom-up cracking propagation in the middle of the specimen, and within a reasonable number of cycles, a 5 × 7 mm^2 transversal notch was created in the middle of the bottom surface of the specimen and a flexible support condition during loading was also created. The defined wheel load per cycle was 700 N and the loading cycles were varied to induce three different levels (high, medium and low) of crack propagation in the specimen. A high damage level meant that the crack spanned the entirety of the beam height, a medium level corresponded to approximately two-thirds of the specimen height, and a low level corresponded to approximately half of the beam height. The medium and low damage levels were obtained at approximately 50% and 25% of the loading cycles needed to see a visible crack on the top surface of the specimen (high level). After loading, the specimens were removed from the mould and adhesive tape was applied on both sides and on the top surface. Then, the specimens were placed upside down and the oil modified with red food coloring liquid pigment (1/1 ratio) was injected with a syringe into the crack along the top surface (bottom surface in the testing position). The specimens were allowed to rest for a minimum of 4 days at room temperature (23 °C) and were then sawn along their length in three equally sized parts for visual inspection. Figure 2b shows the test configuration and the layer system forming the flexible support to the test beam.

3.8. Image-Based Analysis for Assessing Capsule and Rejuvenator Distribution

To assess capsule and rejuvenator distribution in damaged asphalt specimens, the internal surfaces were photographed and the images were analyzed with the ImageJ software package. The color threshold function was used to easily identify capsules and pigmented areas (aggregate and mastic). Highlighting of areas of interest was done using hue saturation and brightness (HSB) color space. Deeper shades of red were selected for the capsules, and tones closer to orange were chosen for pigmented areas outside the capsules. In general, for specimens using capsules made with food coloring, hues between 0 and 7 worked best for capsule material selection, while a range of 8 to 17 picked up most of the red staining. For specimens using capsules with red pellet pigment, hues between 0 and 18 identified capsule material, and 19 to 21 found mastic and aggregate discoloration. The remaining parameters, saturation and brightness, were set to their full range. Figure 3a,b compare the specimen image before and after image treatment to identify the capsule material.

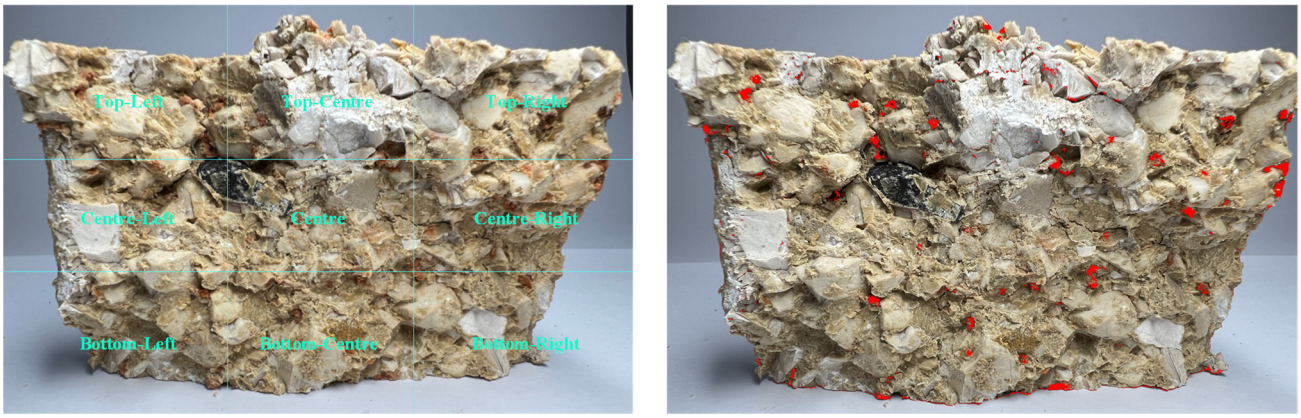

(**a**) (**b**)

Figure 3. Internal view of half of a loaded cylindrical asphalt specimen with capsules (approximately 10 × 6 cm^2): (**a**) original image with a 3 × 3 grid applied; (**b**) color thresholding applied to image.

The areas of interest were classified based on the following criteria:

- *Whole or mostly whole capsules*—Capsules that retained the majority of their volume and whose shape, even if somewhat deformed, was recognizable;
- *Deformed or crushed capsules and capsule remnants*—All these particles had evidence of damage, although it might have occurred at different times. Deformed or crushed capsules are likely to have been damaged during loading, while capsule remnants are more likely to have been created when the specimen was fractured, although these are not mutually exclusive. Even though capsules can release some rejuvenator due to imposed deformation without cracks, these particles indicate areas where loads were high and rejuvenator release was likely;
- *Altered aggregate*—Areas of the aggregate's original white hue have morphed into reddish tones or a darker "oil-stained" white color indicating rejuvenator absorption by the rock;
- *Altered mastic*—Similar to the previous alterations, shifts in the mastic color are a strong indication of the absorption of colored oil in that area. These can be identified by their lighter shades of red when compared to the capsules.

The elements were counted based on a 3 × 3 square grid applied to images (see Figure 3a) to evaluate their distribution in the specimen.

In specimens without capsules in which the pigmented oil was injected into cracks, the ImageJ software was used to measure the distances of oil propagations and crack widths.

4. Results and Analysis

4.1. Modification of Colorless Binder with Pigmented Rejuvenator

4.1.1. Rheological Behavior

Figure 4a shows the variation of the complex shear modulus with the frequency for the colorless binder modified with increasing (non-pigmented) sunflower seed oil content (0–10%) at two temperatures (20 °C and 60 °C). As expected, the modulus was lower for the binder samples tested at 60 °C when compared to the ones tested at 20 °C. Additionally, an increase in oil content resulted in a decrease in complex shear modulus across all frequencies. At the frequency of 1 Hz, the complex modulus of the colorless binder with a 10% oil content was 47.5%, and 67.1% less than that of the non-modified binder at, respectively, 20 °C and 60 °C. To compare the effect of sunflower seed oil on colorless binder and bitumen, Figure 4b plots the complex shear modulus results for the bitumen modified with increasing oil content that was investigated in the study reported in [5]. It is worth mentioning that the bitumen was extracted from a long-term aged bituminous mixture and then modified with the oil to be tested in the DSR. At the same frequency as considered before (1 Hz), the bitumen complex modulus was reduced by 93.4% due to the addition of 10% oil at 20 °C, and by 92.9% at 50 °C. These results show that sunflower seed oil has a significant effect on the rheological behavior of both synthetic and conventional binders. However, in synthetic binder mixtures, the asphalt self-healing mechanisms (flow deformation, wetting and diffusion) are expected to be slower and less effective due to the decreased effect of this rejuvenator on binder rheology [11,23].

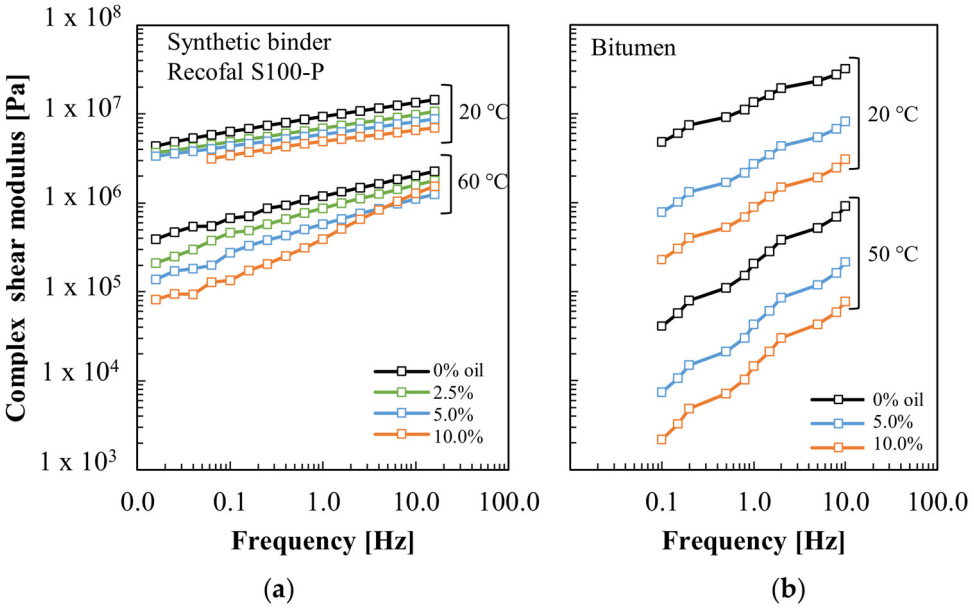

Figure 4. Effect of sunflower seed oil on the complex shear modulus vs. frequency curves: (**a**) colorless binder; (**b**) bitumen (results from [5]).

4.1.2. Binder Pigmentation

Figure 5 shows the influence of sunflower seed oil modified with six pigments on the colorless binder's color. The binder was modified with various oil contents and then spread with a spatula on tracing paper sheets. The oil content, measured by weight, is indicated next to each smear.

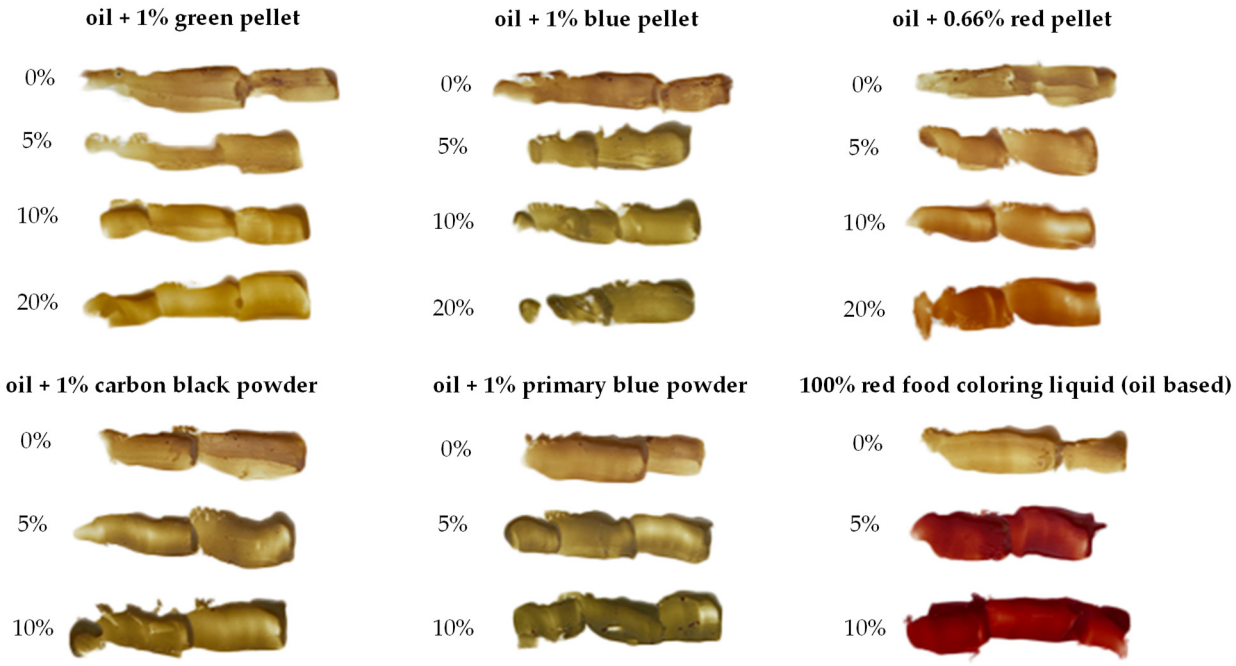

Figure 5. Effect of different pigments on colorless binder color.

The natural color of the synthetic binder varies from yellow to light brown depending on spread thickness. Although the sunflower oil assumed the strong color of pigments used with small contents added (0.66–1.00%), most pigmented oils caused little change in the color of the binder. As regards pigments in pellets (polymer base), the green pellet pigment was by far the worst performer, closely followed by the blue pigment. While the former produced no visible changes, the latter slightly changed the binder hue, but only at high oil concentrations. The red pellet-based oil was deemed to be the best performer out of the three pellet pigments, as the resulting reddish tone was expected to have a higher contrast with the mastic in specimens (with a duller yellow tone than the binder original one).

Black, green and blue powders produced better, but still lacklustre, results. The black oil naturally darkened the binder, but the resulting tones were interpreted to have poor contrast with the mastic and aggregates. Darkening the binder also hampers the distinction between the latter and the dim pores. The red fat-soluble coloring (sunflower oil based) was the best binder color modifier, with minimal concentrations producing very noticeable hue changes.

Based on these results, the two red pigments were selected for use in capsule manufacture.

4.2. Characteristics of Pigmented Rejuvenator Capsules

Most capsules (depicted in Figure 6) had a slightly oval shape, which was due to the production method, i.e., drop-wise extrusion using a funnel. Table 3 presents capsule dimensions for the various batches. Capsules A-1 and B, with the same constituent proportions and different pigments, had similar sizes (approximately 2.38 mm). These results suggest that the pigment does not significantly affect the rejuvenator–alginate emulsion droplets that make the capsules. However, the size of capsules is dependent on different technical aspects of production, e.g., the diameter of the bottom spout of the dropping funnel. Thus, in [22], an average size of 1.7 mm was reported for the calcium capsules containing sunflower oil and very similar constituent ratios.

(**a**) (**b**) (**c**)

Figure 6. Capsules type: (**a**) A-1; (**b**) A-2; (**c**) B.

Table 3. Capsule dimension.

Capsule Batch	Dimension (mm)
A-1	2.36 ± 0.18
A-2	2.85 ± 0.33
B	2.39 ± 0.16

Note: average value ± standard deviation.

As expected, capsules A-2, which were produced with double O/W ratio, were larger (20%), which may make them more adequate for mixtures with larger aggregate sizes and help to increase local rejuvenator volume. It is generally accepted that, in asphalt self-healing, the characteristics of capsules (size, strength, payload, etc.) should be adapted to the specific characteristics of the bituminous mixture and site conditions (environmental, traffic, etc.) [24].

The mechanical behavior of capsules under compressive loading is summarized in Table 4. As expected, the produced capsules were fairly soft, with a yield load and deformation of 20.1–29.2 N and 0.41–0.74 mm, respectively. This yield point was identified as the first interruption (drop) in the load–deformation curve and corresponds to cracks forming in the soft polymer structure. Thereafter, the load continued to grow until most of the rejuvenator had been released and only the polymer structure was crushed between the test plates.

Table 4. Mechanical test results of both heated and unheated capsules.

Capsule Type		Yield Load (N)	Yield Deformation (mm)	Elastic Deformation Slope (N/mm)
A-1	Unheated	28.1 ± 1.8	0.51 ± 0.17	55.2 ± 18.5
	Heated	27.8 ± 4.1	0.41 ± 0.14	68.6 ± 26.0
A-2	Unheated	20.1 ± 3.3	0.61 ± 0.19	32.7 ± 11.4
	Heated	26.6 ± 5.1	0.74 ± 0.25	35.8 ± 14.0
B	Unheated	29.2 ± 2.1	0.58 ± 0.08	50.2 ± 7.8
	Heated	26.9 ± 1.8	0.36 ± 0.13	74.8 ± 28.3

Note: average value ± standard deviation.

In the same way as for the size, capsules A-1 and B had similar mechanical characteristics despite encapsulating different pigmented rejuvenators. Additionally, capsules A-2 were softer because the O/Alg ratio used in production was lower. However, unexpectedly, the three batches of capsules showed similar strength values (26.6–27.8 N) after having been submitted to a heating treatment that simulates asphalt production conditions. Capsules A-1 and B showed a small decrease in strength when compared with unheated capsules, while capsules A-2 showed an increase in strength. The literature [25] mentions that the polymer structure of capsules is affected by depolymerization mechanisms when heated above 100 °C, despite the mass loss of capsules not being very significant (<20%)

at 200 °C [22]. In addition, it was noticed that all heated capsules had a fainter color tone than unheated capsules, which can make their identification in asphalt specimens harder.

To understand the effect of pigments on oil release, some capsules were placed on white paper sheets and then fully compressed. Figure 7 compares the capsule "print" after several days. It is clear that the pigmented rejuvenator was released when the capsule was crushed, and a large stain of clear oil was formed around the inner pigmented area. The latter is likely the result of the capillary flow across the porous media, drawing rejuvenator from the capsule and into the paper, while filtering out the pigment along the flow course. Naturally, the rejuvenator proportion in capsules is proportional to the capsule size, and, as such, larger capsules originated larger stained areas, as seen for capsules A-2 (Figure 7b). Capsules A-1 showed a larger proportion of pigmented area to the total stained area than capsules B, which share the proportion of the constituents. However, the mechanisms requiring further investigation, the capsule damage and the rejuvenator release, are different in the asphalt mixture.

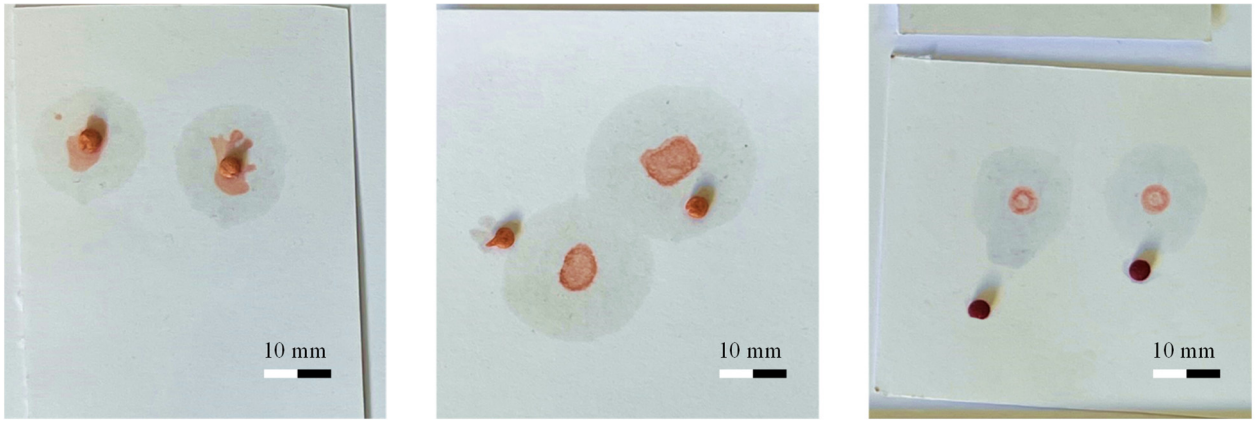

(**a**) (**b**) (**c**)

Figure 7. Crushed calcium alginate capsule: (**a**) A-1; (**b**) A-2; (**c**) B.

The capsule color hue remained very strong after being crushed, which suggests that part of the pigment is bonded to the capsule polymer structure and is not available for asphalt pigmentation. Although not ideal, since a reasonable amount of pigment was still released by the capsules, these were incorporated into asphalt to proceed with the study of asphalt self-healing with encapsulated pigmented rejuvenator.

4.3. Asphalt Specimens with Pigmented Oil Capsules

Figure 8 compares the internal structures of the two bituminous mixtures made with paving-grade bitumen and synthetic colorless binder side by side. The cylindrical specimens were sawn in vertical and horizontal directions for comparison purposes. A similar coarse aggregate structure with black and colorless binders could be observed for the asphalt concrete and the stone mastic asphalt, with quite different aggregate gradations. Although the specimens with the colorless binder may initially appear to have fewer small aggregates between the larger ones, or more mastic, this is a matter of contrast. Upon closer inspection, the mastic in the colorless binder samples reveals many small aggregates, as expected, the shape and color of which appear to be masked by the surrounding binder.

Considering that the internal structure of conventional bituminous mixtures could be mostly reproduced using a colorless binder, mixtures were produced containing pigmented capsules. Figure 9 shows the internal sawed surface of specimens of the two bituminous mixtures (AC 14 and SMA 11) with 2% of capsules of type A-2. Capsules can be seen on cut surfaces, but while certainly visible, the capsules containing the rejuvenator colored with red pellets were sometimes hard to distinguish. According to the visual observation, the capsules were generally located next to coarse aggregates, were locked in the asphalt

structure and varied in shape and condition. Additionally, most cylindrical specimens appeared to have an even distribution of capsules. However, it should be noted that this visual analysis is affected by the sawing process (approximately 5 mm of thickness is lost during this process). Hence, in the same way as discussed before for the experiment of rejuvenator release on paper, sawed specimens started to display clear rejuvenator stains around their capsules hours after sawing. These rejuvenator stains were likely formed by the capillary action that drew the rejuvenator out of the capsules, while most of the pigment was filtered during this process.

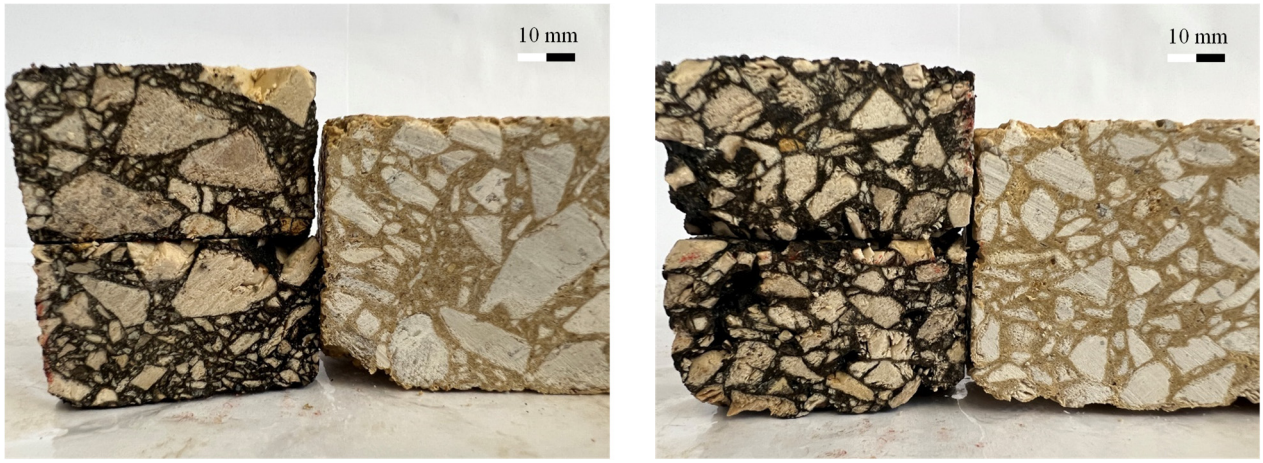

(**a**) (**b**)

Figure 8. Asphalt specimens with bitumen and colorless binder: (**a**) AC 14; (**b**) SMA 11.

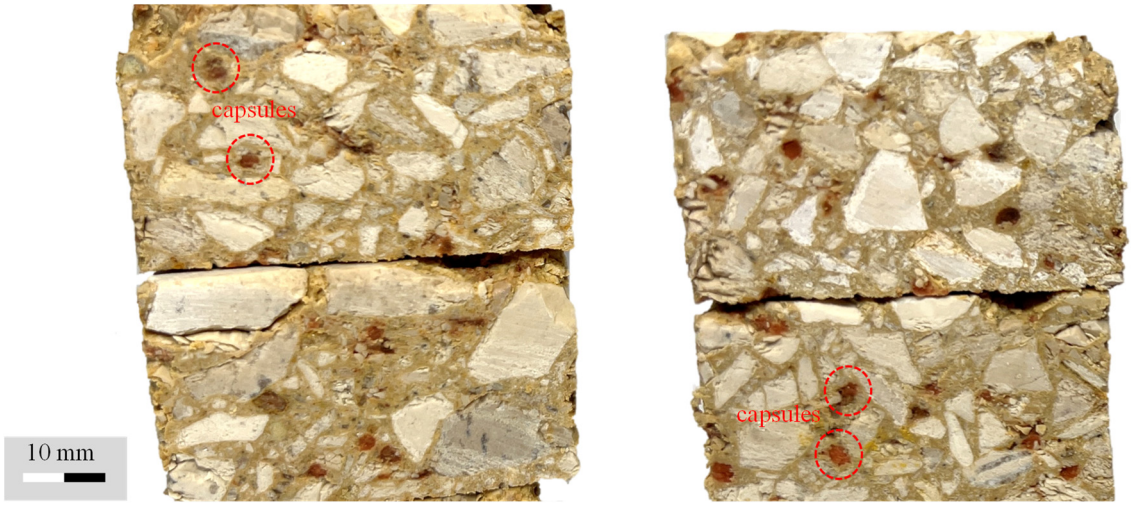

(**a**) (**b**)

Figure 9. Internal structure of asphalt specimens with encapsulated rejuvenators (A-2, 2%w): (**a**) AC 14; (**b**) SMA 11.

4.4. Dispersion of Pigmented Rejuvenator in Loaded Asphalt Specimens with Capsules

Following the effective fabrication of clear bituminous mixtures using a colorless binder and with a pigmented encapsulated agent, the asphalt specimens with different capsules were subjected to the confined mechanical compressive loading shown in Figure 2a to study capsule release and the dispersion of pigmented rejuvenator in asphalt. This procedure was implemented because, as reported in [16], the release efficiency of calcium alginate capsules is higher when the capsules are harder compressed between the aggregates. However, it should be mentioned that in the asphalt self-healing with encapsulated

rejuvenator technique, these capsules will remain inactive in an asphalt road for several years until an external factor, e.g., loading, triggers their breakage and the rejuvenators dissolve the bitumen around the microcapsules. Then, the binder can easily flow into the cracks and self-healing is accelerated. This will allow for preserving the infrastructure for longer periods without maintenance needs, and help in achieving sustainable maintenance-free asphalt roads.

The specimens were inspected internally after resting for a day at room temperature until reaching equilibrium conditions. Figure 10 presents in radar plots the distribution of capsule and capsule–asphalt interactions in the analyzed internal surfaces (approximately 10×6 cm^2) of specimens, and the total count of relevant elements is listed in Table 5. As described in Section 3.8, a 3×3 grid was used in the measurements (see Figure 3) and the following relevant elements were considered: (i) whole/mostly whole capsules; (ii) deformed/crushed capsules, including capsule remnants; (iii) altered (pigmented/stained aggregate); and (iv) altered (pigmented) mastic.

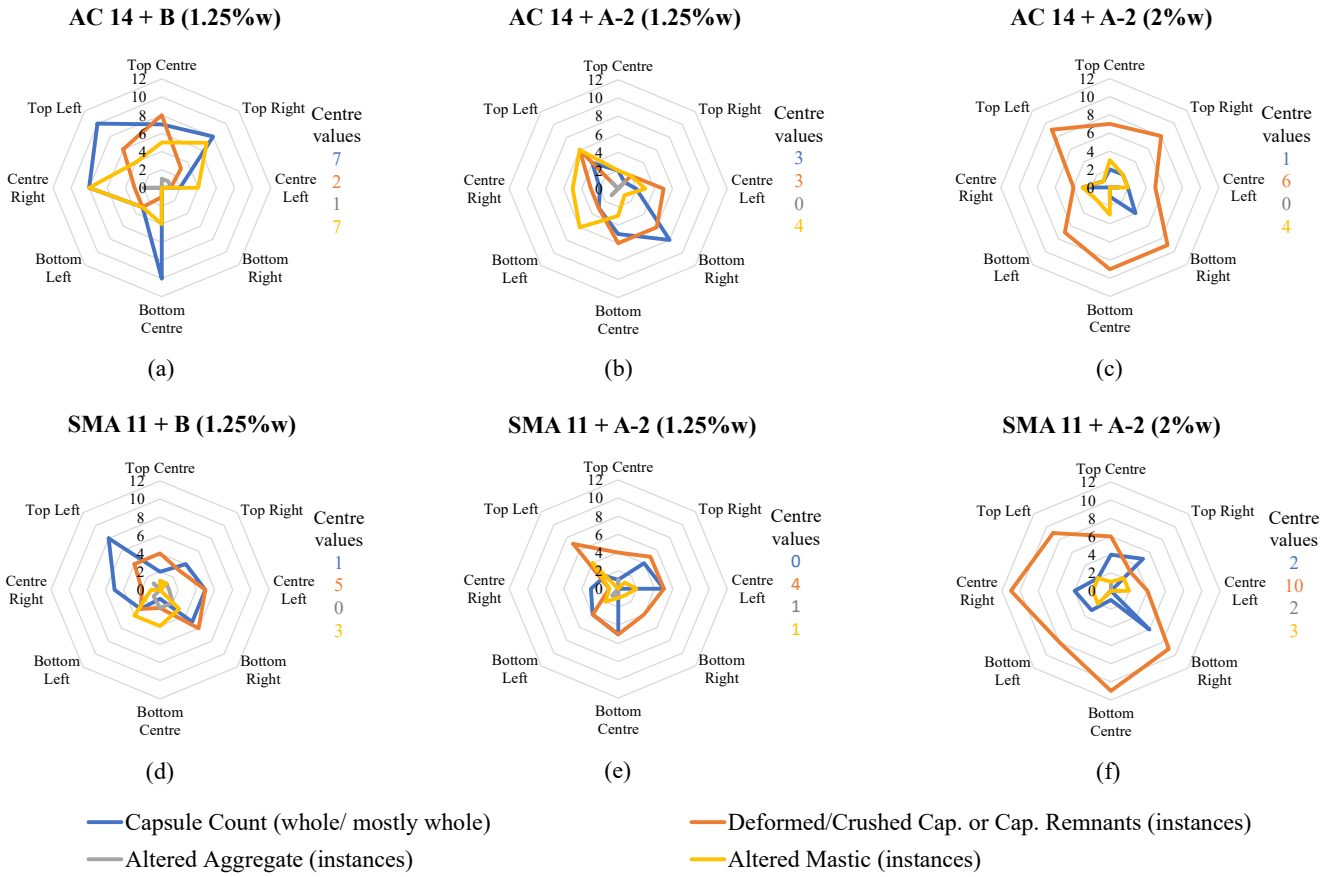

Figure 10. Distribution of capsule and capsule/asphalt interactions in the loaded asphalt specimens: (**a**) AC 14 + B (1.25%w); (**b**) AC 14 + A-2 (1.25%w); (**c**) AC 14 + A-2 (2%w); (**d**) SMA 11 14 + B (1.25%w); (**e**) SMA 11 + A-2 (1.25%w); (**f**) SMA 11 + A-2 (2%w).

In general, the number of capsules (both whole and damaged) was much higher than the number of mastic and aggregate elements affected by the oil encapsulated in calcium alginate capsules. This indicates that loading was insufficient to break capsules, the pigmented oil released from capsules was not very high, or part of the pigment was entrapped in the capsules. Hence, as illustrated in Figure 3 (Section 3.8), the color of the internal surface of the specimen was not significantly different from that of unloaded specimens, as could be expected if all the pigment had been released. The asphalt specimens showed significant damage, which allowed for breaking them in half with a chisel and hammer. As anticipated, the number of altered aggregates was small, and given that

the aggregates were covered by mastic film, the oil was less likely to affect the aggregate than the mastic surrounding it. Nevertheless, some cracks induced by loading may have developed in the mastic–aggregate interface, leading the oil from the capsules to reach the mineral aggregates.

Table 5. Summary of image-based analysis of the loaded asphalt specimens with capsules.

	AC 14			SMA 11		
	B (1.25%w)	**A-2 (1.25%w)**	**A-2 (2.0%w)**	**B (1.25%w)**	**A-2 (1.25%w)**	**A-2 (2.0%w)**
Capsule (whole/mostly whole)	59	30	16	34	24	27
Deformed/crushed capsule	27	34	64	34	39	71
Altered aggregate	6	3	1	8	4	5
Altered mastic	45	32	20	17	13	14

Note: total count values.

Nevertheless, the results of the image-based analysis show that the effectiveness of asphalt self-healing based on encapsulated rejuvenators is affected by numerous factors, such as the capsule type and content, as well as the bituminous mixture. The radar plots show no effect of the position on any of the measures, to which the loading mode (confined compression) possibly contributes.

As expected, the proportion of damaged to intact capsules increased in specimens with weaker capsules (A-2 versus B) and with more added capsules (2.00% versus 1.25%w). For instance, in SMA 11, the proportions of damaged capsules were 50%, 62% and 72% for mixtures with B (1.25%w), A-2 (1.25%w) and A-2 (2.00%w), respectively. The equivalent values for AC 14 were 46%, 53% and 80%. However, the number of total capsules measured for AC 14 with B capsules was much higher than expected.

Another unexpected finding was that the number of pigmented mastic instances varied in opposition to the ratio of damaged to intact capsules. For instance, in AC 14 with A-2 capsules the number of pigmented mastic instances decreased from 32 to 20, while the ratio of damaged capsules increased from 53% to 80%. For the analysis of the results, it is necessary to consider the different effects of the two pigments on the rejuvenator and on the colorless binder, together with the resulting difficulties in the visual analysis even with the aid of image treatment software. The red liquid pigment demonstrated a substantially greater coloring performance when compared to the red pellets, meaning that any release of it, even in limited amounts, is more likely to produce visible staining than the pellet-colored oil, leading to the differences in instances of dyed aggregate and mastic. Therefore, it is likely that not all instances of altered mastic were identified in specimens with capsules type A-2, and that some instances of altered mastic were incorrectly identified as capsule remnants in the specimens with greater capsule content (2.00%w).

However, for both types of capsules used, the number of pigmented mastic instances was significantly greater in AC 14. It is commonly accepted that the aggregate gradation of bituminous mixtures affects the damage extent and the evolution with loading due to the differences in the interlocking of mineral particles and the binder thickness around particles [26,27]. Therefore, the aggregate gradation is likely to affect capsule damage occurrence and, in the case of calcium alginate capsules, which hold the rejuvenator in a multi-cavity structure, the load transfer between aggregate particles and capsules in contact is extremely important.

To help clarify doubts as regards the effect of different pigmented capsules on different bituminous mixtures, the specimens were observed under a binocular microscope. Figure 11 illustrates the differences between capsule types A-2 and B, and the ability of encapsulated pigmented oil to modify the near mastic. The color hue difference between capsules A-2 and the surrounding mastic is very small (see Figure 11a), making it very hard to define the capsule limits. Differently, in Figure 11b, the capsule limits and the pigmented mastic can be easily distinguished. It should be noted that despite these being individual examples

representative of the most common occurrences in the specimens, there were some instances in all the samples where no rejuvenator release could be found around capsules of type B, and rejuvenator or large amounts of discoloration were observed in capsules of type A-2.

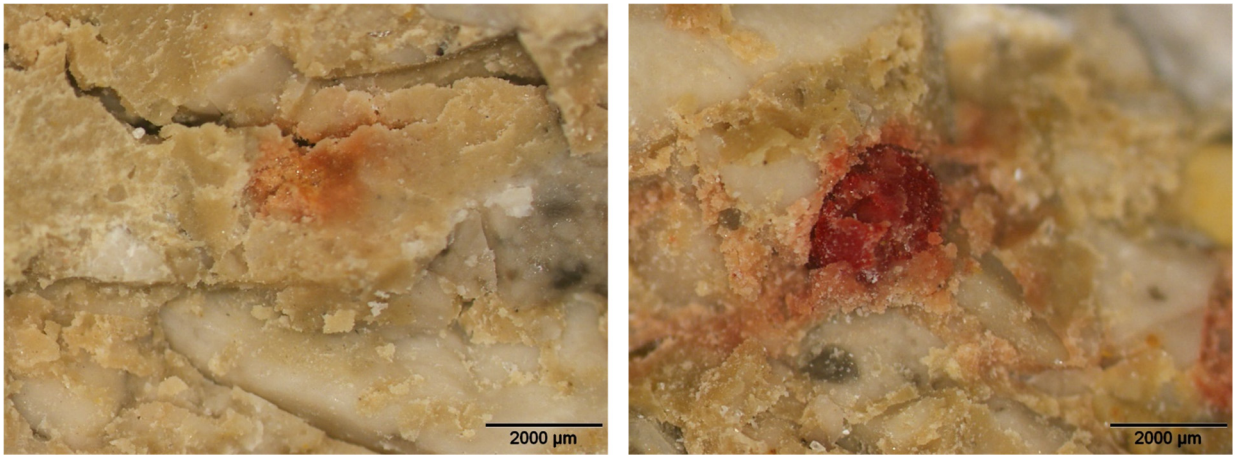

(**a**) (**b**)

Figure 11. Staining of AC 14 mastic around capsule type (**a**) A-2 and (**b**) B.

In addition, Figure 12 illustrates the difference in mastic pigmentation in specimens of AC 14 and SMA 11 with capsules of type B. There was more mastic pigmentation in AC 14, which confirms the results shown in Table 5 and Figure 10. This is most likely due to the arrangement of the capsules within the aggregate structure. In the AC mixture, the capsules appeared to have a random distribution, often surrounded by aggregates of various sizes. Differently, in the SMA mixture, it is noticeable that the capsules often fitted into pockets of smaller aggregates and mastic between coarse aggregates. Hence, to achieve effective asphalt self-healing with encapsulated rejuvenator in different bituminous mixtures applied in different conditions (traffic, environmental, etc.), the capsules' properties (size, mechanical, and payload) have to be adjusted to the particular situations.

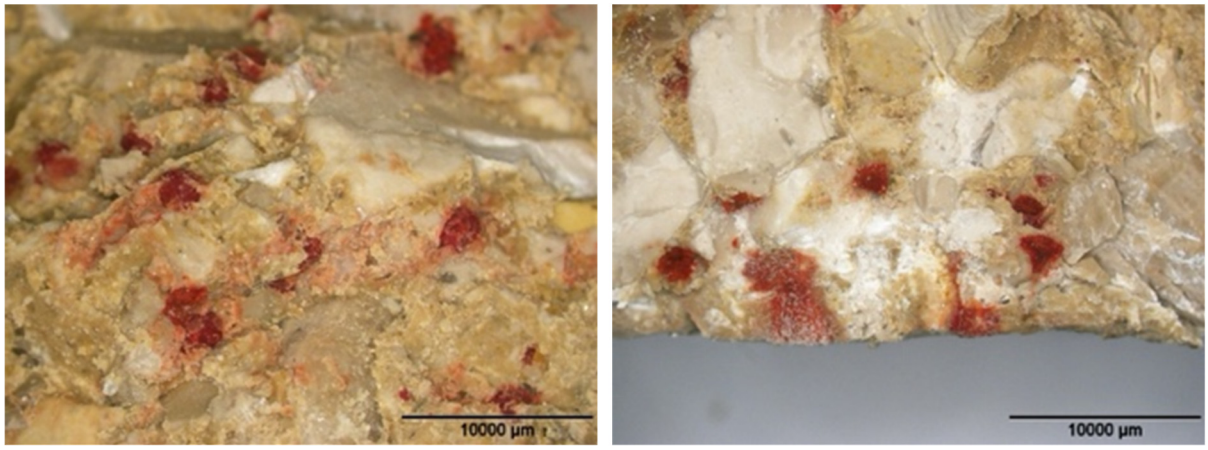

(**a**) (**b**)

Figure 12. Mastic pigmentation due to type B capsules in loaded specimens: (**a**) AC 14; (**b**) SMA 11.

4.5. Analysis of Oil Propagation in Asphalt Beams Subjected to Repeated Flexion

Figure 13 presents images of the interior (central portion) of the asphalt specimens that were submitted to different loading cycles and injected with pigmented rejuvenator (50/50 red food coloring liquid pigment and sunflower seed oil). The specimens were rested for 4 days at room temperature before sawing. It should be noted that the images

show the specimens in the positions in which they were loaded, but they were positioned upside down during rejuvenator injection and resting. This means that the rejuvenator propagated downwards due to gravity. Additionally, the volume of rejuvenator was adjusted to simulate the number of capsules that could be affected in the damaged zone if the bituminous mixture contained encapsulated rejuvenators.

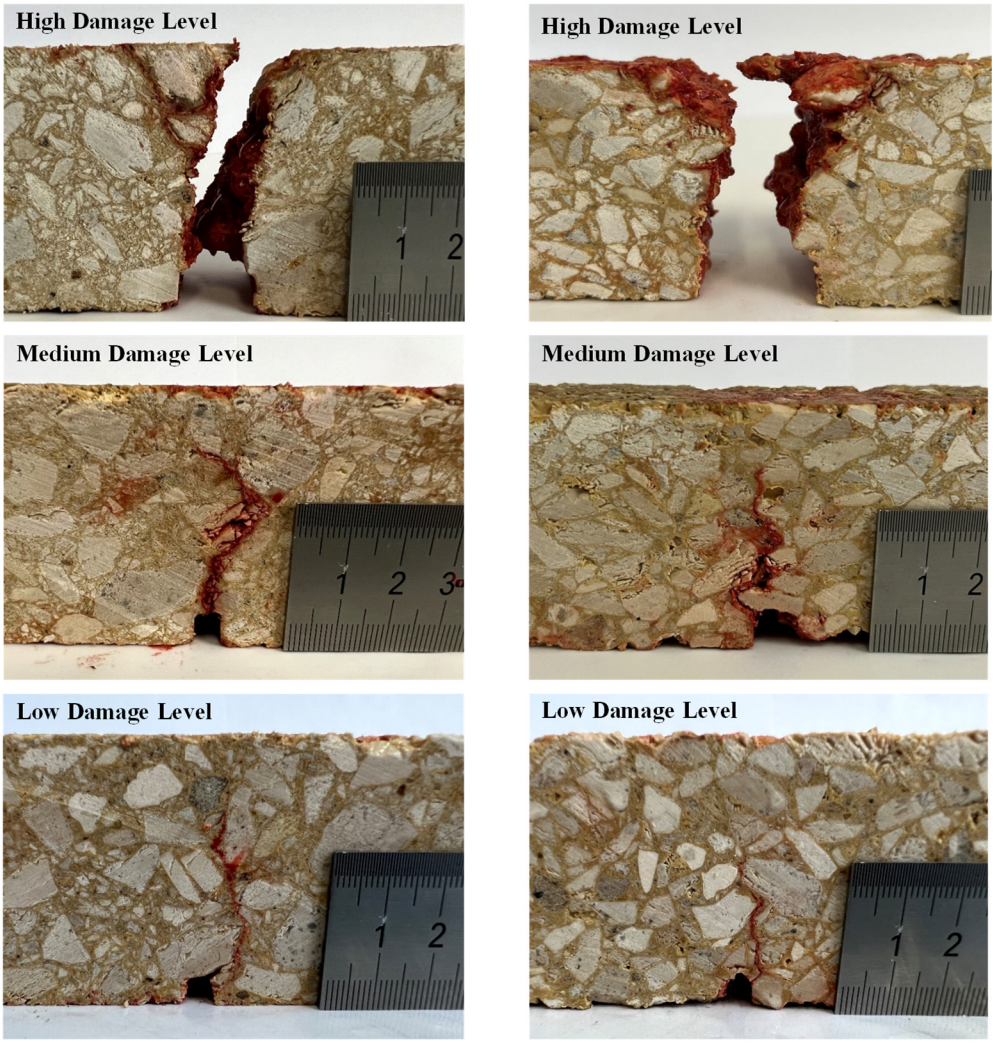

Figure 13. Pigmented rejuvenator dispersion after 5 days in fatigue-damaged asphalt specimens: (**a**) AC 14; (**b**) SMA 11.

At the high damage level, the cracks extended fully over the height and width of the specimens, and they could be separated into two parts. Some important secondary cracks were observed, which derived from the main crack. Crack opening width varied mostly between 0.2 and 0.5 mm. For the intermediate level, in AC 14, the crack was 33–49 mm long with an average opening width of 0.23 mm, and in SMA 11, it was 25–38 mm long with an average width of 0.35 mm. For the lowest damage level, in AC 14, the crack was 35–38 mm long with an average opening width of 0.16 mm, and in SMA 11, it was 13–31 mm long with an average opening width of 0.13 mm. Hence, the testing procedure used induced different levels of damage as intended, although the cracking condition was not identical in the two bituminous mixtures for the same level. Clearly, crack opening and growth highly depend on aggregate size and gradation.

In general, the pigmented rejuvenator was able to flow along both the main crack and the smaller secondary cracks derived from the main one. In the case of the most damaged

specimens, it was observed that the rejuvenator filled cracks around the large aggregate particles sitting on the opposite side to where the rejuvenator was injected, and some cracks filled with pigmented rejuvenator were not connected to the main crack in the cut surface. Capillary flow was most likely necessary to reach these crack tips far from the main crack. Clearly, the amount of rejuvenator filling the crack diminished as the cracks became thinner and less rejuvenator was injected in the less damaged specimens. Thus, in the case of AC 14 loaded to the intermediate damage level, no pigmentation was observed in the last 14 mm of the main crack (49 mm), possibly because it was too narrow.

Referring to the diffusion of the pigmented rejuvenator in mastic and aggregates, a color change was generally observed in the area closest to the crack (see Figure 14). Next to the crack surface, the materials assumed a red color, and then a second region with a darker hue than the natural material color. This suggests that the pigment particles separated from the base rejuvenator along the diffusion path. The width of the region close to cracks changed by the rejuvenator varied widely in the specimens, but was generally larger in the wider parts of the cracks. It is possible that the pigmented rejuvenator accumulated in the wider parts of the cracks because these were closer to the rejuvenator injection point. It is noteworthy that on the day following the cut and inspection, the asphalt surfaces displayed bands of rejuvenator-stained aggregate and mastic on either sides of the main crack. This staining did not show any red hue. It is likely that, after sawing, the aggregate and mastic were able to come into contact with the thin film of rejuvenator present in the primary crack, having drawn some of it out. It is plausible that due to pore size, the pigment particles were filtered out of this rejuvenator.

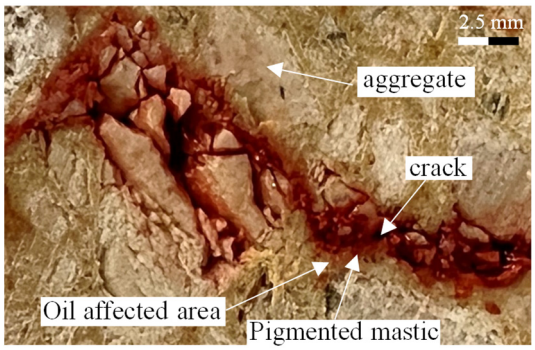

Figure 14. Rejuvenator (sunflower seed oil) diffusion near the crack (AC 14, medium damage level).

4.6. Colorless Binder Solubility in Rejuvenator at Room Temperature

Although the sunflower seed oil (rejuvenator) effectively decreased the stiffness of the colorless binder, the analysis of damaged asphalt specimens, with the oil present in capsules or the oil injected in the cracks, showed that the pigmented oil had a small impact. To study the interaction of sunflower oil with the colorless binder at intermediate pavement temperatures, a binder solubility test was implemented, which was based on the European procedure for the determination of affinity between aggregate and bitumen (EN 12697-11:2020).

Figure 15 depicts the appearance of the two mixtures over the course of the test. The aggregates coated with traditional bitumen lost most of their coating to the oil, as the aggregate gradually became more exposed over the testing time. In the mixture using the colorless binder, differences in binder coverage were naturally harder to identify. Some aggregates showed darker areas where the binder happened to pool. However, in general, there was a difference in coating between 0 and 48 h. The areas where binder pooled appeared smaller, and the zones where a thinner layer was present appeared whiter, revealing the aggregate's color. Hence, the oil in which the mixtures were submerged also changed (see Figure 15c). In the case of the sample with bitumen, the oil immediately became opaque and dark as soon as the aggregate pouch was lifted for the first weighing.

The oil in contact with the colorless binder mixture did not display sudden changes, but gradually became more orange as the test went on, resembling the synthetic binder color.

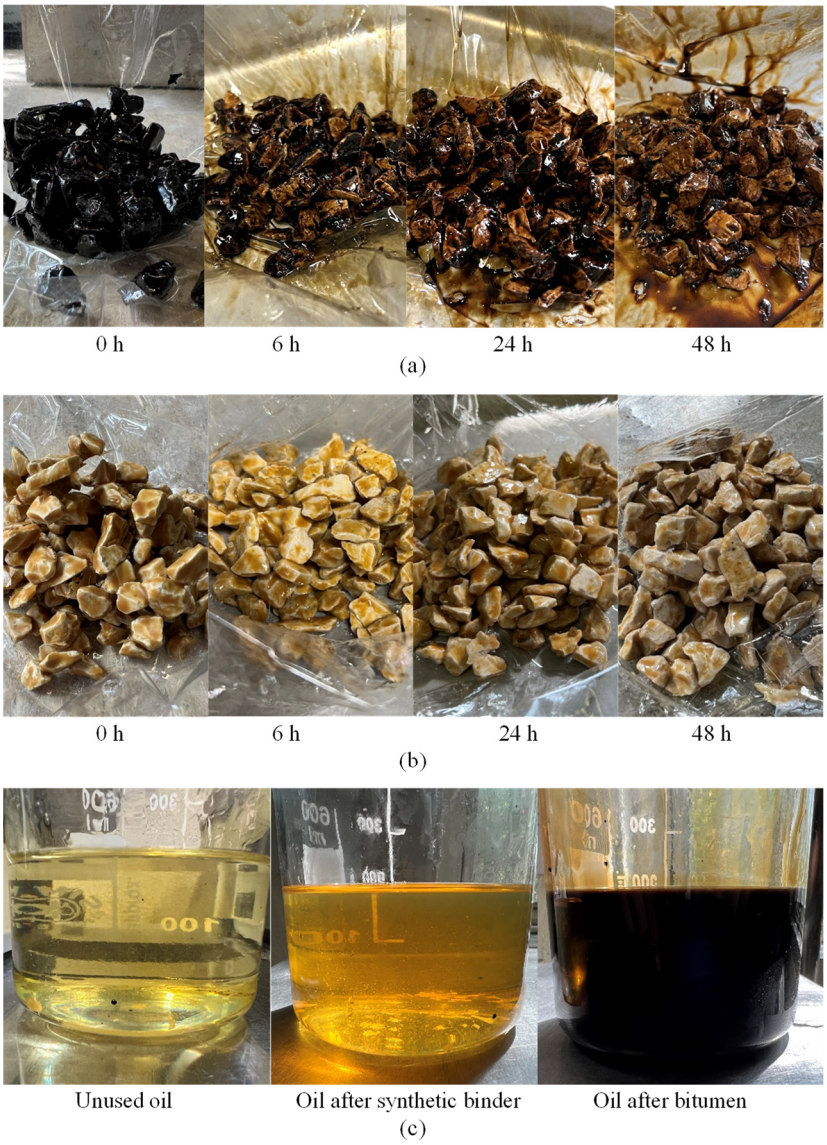

Figure 15. Binder solubility test: (**a**) aggregate–bitumen mixture; (**b**) aggregate–colorless binder mixture; (**c**) sunflower oil.

The evolution in the mass of each mixture was also monitored (see Table 6). The recorded masses were only intended for comparison between the two samples, as the oil was not fully drained out of the aggregate bulk. After the initial measurement, the aggregates were coated with oil. At 48 h, after a standard weighing procedure, the aggregates were spread out on strainers until oil drops stopped forming. This left only a thin coating of oil on the surface of the aggregates, which could not be removed without disturbing the remaining binder film. The relative mass variation (ΔB) was calculated as

$$\Delta B = \frac{{M_{Agg+B}}^t - {M_{Agg}}^0 - {M_B}^0}{{M_B}^0} \times 100, \quad (1)$$

where ${M_{Agg+B}}^t$ is the aggregate and binder mass at time t, and ${M_{Agg}}^0$ and ${M_B}^0$ are the masses of aggregate and binder used in the experiment. The mass loss of bitumen-coated aggregates is remarkably high (48%). In opposition, while some loss was visually identified

in the colorless binder, the sample mass still showed an increase relative to the start, which means that the binder loss was not enough to offset the mass gain from the oil coating/absorption. Intermediate measurements showed a clear downward trend in the mass of the sample with bitumen, while the mass of the colorless binder mix mostly remained stable. Therefore, this demonstrates that the effect of sunflower seed oil on the colorless binder was small at room temperature.

Table 6. Mixture mass over the course of the binder experiment.

Time (h)	Aggregate+Binder Mass, $M_{Agg+B}{}^{t}$ (g)		Relative Mass Variation,ΔB (%)	
	Colorless Binder	Bitumen	Colorless Binder	Bitumen
Initial (dry)	160.63	157.27	0%	0%
1	167.53	165.14	+69%	+110%
2	168.09	163.36	+74%	+85%
3	167.64	162.18	+70%	+68%
4	167.30	160.98	+67%	+52%
5	168.10	160.21	+74%	+41%
6	167.80	159.29	+71%	+28%
25	168.56	160.43	+79%	+44%
26	166.88	159.38	+62%	+29%
48	169.31	159.99	+87%	+38%
48 (drained)	161.97	153.81	+13%	−48%

5. Conclusions

Universal access to affordable, reliable, sustainable, and modern transport systems is one of the foremost commitments of the 2030 Agenda. In high-income countries, there is a deficit of investment directed to properly maintain current infrastructures, whereas low-income countries aim to expand their transportation networks. Hence, new and advanced technological solutions for the planning, design, construction and maintenance of transport infrastructures are needed to comply with the agreed climate and sustainable development goals. Asphalt self-healing with encapsulated rejuvenator is a bio-inspired system used in roads and runways, which by being able to self-repair, will not require normal maintenance and will have an extended service life. However, this technology is still at an early stage, and new numerical and experimental approaches are needed for its development.

This paper assessed and demonstrated the feasibility of an innovative method of studying asphalt self-healing, which consists of visually inspecting the effect of encapsulated rejuvenators using a colorless binder and pigmented rejuvenator. Several experiments were conducted to understand the behaviors and interactions of the various components of these mixtures. Overall, this study showed that the proposed methodology is capable of giving meaningful microstructural information on the interaction between encapsulated rejuvenators and the bituminous mixture components, which can eventually assist in the interpretation of experimental testing results regarding bulk asphalt materials. Furthermore, the most important issues for the success of the visual inspection are analyzed and discussed. The following specific conclusions have also been drawn from the study:

- It is possible to produce pigmented rejuvenators that markedly change the colorless binder's hue, and it is also possible to produce calcium alginate capsules containing these oils. However, pigment release from loaded calcium alginate capsules, while certainly present, is limited compared to rejuvenator release;
- It is possible to produce light-colored bituminous mixtures containing encapsulated rejuvenators in which they are evident. Colorless rejuvenator release in unloaded cylindrical specimens was identified many hours after sawing (and the associated damaging of the cut capsules), but not immediately after. This suggests that only small amounts of oil were released due to mixing and compaction;
- In loaded specimens, a positive correlation was found between capsule concentration and the number of capsules and capsule fragments. A higher proportion of broken

capsules was found in the mixtures with higher capsule concentrations (in AC14, variation from 53% to 80% with 1.25% and 2.00% capsules). The ratio of crushed capsules and capsule fragments to whole/mostly whole capsules was significantly lower in the case of capsules made with food coloring (46% and 50% with B type versus 53% and 62% with A-2 type), which had a higher proportion of sodium alginate in their composition and should therefore have had higher compressive strength. The amount of staining was found to be higher in asphalt concrete specimens (average of 32 instances) than in stone mastic asphalt ones (average of 15 instances);

- In asphalt beams, to which colored rejuvenator was directly added, the rejuvenator was able to propagate through most of the visible cracks, even when their width was very small (opening width less than 0.2 mm). The rejuvenator was also able to extend across long cracks. However, rejuvenator diffusion in clear asphalt was found to be limited;
- The sunflower seed oil's effect on the colorless binder was different from that on the bitumen. The oil reduced to a lower extent the complex shear modulus of the colorless binder (for a 10% oil content and at 20 °C, a 47.5% decrease was seen, versus 92.9% for an aged bitumen). Additionally, the coated aggregates showed noticeably lower binder loss when immersed in the oil. The bitumen-coated aggregates showed a 48% bitumen mass decrease, while the colorless binder loss did not surpass the additional oil adherent to the mixture (+13%).

Finally, it is noteworthy that these findings are highly dependent on the specific materials used, and that the visual inspection results were conditioned by the limited effect of the sunflower seed oil on the colorless binder and by the barrier effect of the capsule's polymer structure on the pigment. Therefore, the research team intends to evaluate different rejuvenators, pigments and encapsulation systems, and the interaction between these constituents. The usage of dyes instead of pigments might be particularly effective.

Author Contributions: Conceptualization, R.M. and A.C.F.; methodology, R.M. and A.C.F.; validation, R.M. and A.C.F.; formal analysis, T.R., R.M., J.C. and A.C.F.; investigation, T.R., A.C.F., M.S.-d.-C., J.C., V.C. and R.M.; resources, T.R., R.M. and A.C.F.; writing—original draft preparation, T.R., A.C.F., M.S.-d.-C. and R.M.; writing—review and editing, T.R., A.C.F., M.S.-d.-C., J.C. and R.M.; supervision, R.M.; All authors have read and agreed to the published version of the manuscript.

Funding: This work was financed by national funds from FCT—*Fundação para a Ciência e a Tecnologia*, I.P., in the scope of the projects LA/P/0037/2020, UIDP/50025/2020 and UIDB/50025/2020 of the Associate Laboratory Institute of Nanostructures, Nanomodelling and Nanofabrication—i3N, and project UIDB/04625/2020 of the CERIS—Civil Engineering Research and Innovation for Sustainability.

Institutional Review Board Statement: Not applicable.

Informed Consent Statement: Not applicable.

Data Availability Statement: Not applicable.

Acknowledgments: The authors would like to acknowledge the support given to this research by REPSOL and RAVAGO CHEMICALS, providing the binder and the red pellet pigment, respectively.

Conflicts of Interest: The authors declare no conflict of interest.

References

1. Kowalski, K.J.; Bańkowski, W.; Król, J.B.; Andersen, B.H.; Komkova, A.; Casado Barrasa, R. Practical Application of Sustainable Road Structure: Mechanical and Environmental Approach. *Appl. Sci.* **2022**, *12*, 11914. [CrossRef]
2. ASCE. *2017 Infrastructure Report Card*; American Society of Civil Engineers: Reston, VA, USA, 2017.
3. Ferreira, A.; Micaelo, R.; Souza, R. Cracking Models for Use in Pavement Maintenance Management. In *Cracking Models for Use in Pavement Maintenance Management*; RILEM Bookseries; Springer: Dordrecht, The Netherlands, 2012; Volume 4.
4. EC. *The European Green Deal, COM(2019) 640 Final*; European Commission: Brussels, Belgium, 2019.
5. Micaelo, R.; Al-Mansoori, T.; Garcia, A. Study of the Mechanical Properties and Self-Healing Ability of Asphalt Mixture Containing Calcium-Alginate Capsules. *Constr. Build. Mater.* **2016**, *123*, 734–744. [CrossRef]

6. Read, J.; Whiteoak, D. *The Sell Bitumen Handbook*, 5th ed.; Thomas Telford Publishing: London, UK, 2003; ISBN 0-7277-3220-X.
7. Xu, S.; García, A.; Su, J.; Liu, Q.; Tabaković, A.; Schlangen, E. Self-Healing Asphalt Review: From Idea to Practice. *Adv. Mater. Interfaces* **2018**, *5*, 1800536. [CrossRef]
8. García, Á.; Schlangen, E.; van de Ven, M. Properties of Capsules Containing Rejuvenators for Their Use in Asphalt Concrete. *Fuel* **2011**, *90*, 583–591. [CrossRef]
9. Garcia, A.; Bueno, M.; Norambuena-Contreras, J.; Liu, Q.; Partl, M. The Model for Induction-Healing Asphalt Concrete. In *Asphalt Pavements*; CRC Press: Boca Raton, FL, USA, 2014; pp. 1431–1440, ISBN 978-1-138-02693-3.
10. Xu, S. Self-Healing Porous Asphalt: A Combination of Encapsulated Rejuvenator and Induction Heating. Ph.D. Thesis, Delft University of Technology, Delft, The Netherlands, 2020.
11. Varma, R.; Balieu, R.; Kringos, N. A State-of-the-Art Review on Self-Healing in Asphalt Materials: Mechanical Testing and Analysis Approaches. *Constr. Build. Mater.* **2021**, *310*, 125197. [CrossRef]
12. Qiu, J.; van de Ven, M.F.C.; Wu, S.P.; Yu, J.Y.; Molenaar, A.A.A. Investigating Self Healing Behaviour of Pure Bitumen Using Dynamic Shear Rheometer. *Fuel* **2011**, *90*, 2710–2720. [CrossRef]
13. Gonzalez-Torre, I.; Norambuena-Contreras, J. Recent Advances on Self-Healing of Bituminous Materials by the Action of Encapsulated Rejuvenators. *Constr. Build. Mater.* **2020**, *258*, 119568. [CrossRef]
14. Qiu, J. Self-Healing of Asphalt Mixtures, towards a Better Understanding. PhD Thesis, Delft University of Technology, Delft, The Netherlands, 2012.
15. Al-Mansoori, T.; Micaelo, R.; Artamendi, I.; Norambuena-Contreras, J.; Garcia, A. Microcapsules for Self-Healing of Asphalt Mixture without Compromising Mechanical Performance. *Constr. Build. Mater.* **2017**, *155*, 1091–1100. [CrossRef]
16. Ruiz-Riancho, N.; Tahseen, S.; Gracia, A.; Grossegger, D.; Hudson-Griffiths, R. Optimisation of Self-Healing Properties for Asphalts Containing Encapsulated Oil to Mitigate Reflective Cracking and Maximize Skid and Rutting Resistance. *Constr. Build. Mater.* **2021**, *300*, 123879. [CrossRef]
17. Karlsson, R.; Isacsson, U. Application of FTIR-ATR to Characterization of Bitumen Rejuvenator Diffusion. *J. Mater. Civ. Eng.* **2003**, *15*, 157–165. [CrossRef]
18. Norambuena-Contreras, J.; Liu, Q.; Zhang, L.; Wu, S.; Yalcin, E.; Garcia, A. Influence of Encapsulated Sunflower Oil on the Mechanical and Self-Healing Properties of Dense-Graded Asphalt Mixtures. *Mater. Struct.* **2019**, *52*, 78. [CrossRef]
19. Zhang, L.; Zheng, G.; Zhang, K.; Wang, Y.; Chen, C.; Zhao, L.; Xu, J.; Liu, X.; Wang, L.; Tan, Y.; et al. Study on the Extraction of CT Images with Non-Uniform Illumination for the Microstructure of Asphalt Mixture. *Materials* **2022**, *15*, 7364. [CrossRef] [PubMed]
20. Segundo, I.R.; Freitas, E.; Branco, V.T.F.C.; Landi, S.; Costa, M.F.; Carneiro, J.O. Review and Analysis of Advances in Functionalized, Smart, and Multifunctional Asphalt Mixtures. *Renew. Sustain. Energy Rev.* **2021**, *151*, 111552. [CrossRef]
21. Micaelo, R.; Freire, A.C.; Pereira, G. Asphalt Self-Healing with Encapsulated Rejuvenators: Effect of Calcium-Alginate Capsules on Stiffness, Fatigue and Rutting Properties. *Mater. Struct.* **2020**, *53*, 20. [CrossRef]
22. Al-Mansoori, T.; Norambuena-Contreras, J.; Micaelo, R.; Garcia, A. Self-Healing of Asphalt Mastic by the Action of Polymeric Capsules Containing Rejuvenators. *Constr. Build. Mater.* **2018**, *161*, 330–339. [CrossRef]
23. García, Á. Self-Healing of Open Cracks in Asphalt Mastic. *Fuel* **2012**, *93*, 264–272. [CrossRef]
24. Inozemtcev, S.; Jelagin, D.; Korolev, E.; Fadil, H.; Partl, M.N.; Do Trong, T. Experimental and Numerical Study on SMA Modified with an Encapsulated Polymeric Healing Agent. *Mater. Struct.* **2022**, *55*, 230. [CrossRef]
25. Leo, W.J.; McLoughlin, A.J.; Malone, D.M. Effects of Sterilization Treatments on Some Properties of Alginate Solutions and Gels. *Biotechnol. Prog.* **1990**, *6*, 51–53. [CrossRef] [PubMed]
26. Sousa, J.B.; Pais, J.C.; Prates, M.; Barros, R.; Langlois, P.; Leclerc, A.-M. Effect of Aggregate Gradation on Fatigue Life of Asphalt Concrete Mixes. *Transp. Res. Rec.* **1998**, *1630*, 62–68. [CrossRef]
27. Hunter, R.N.; Andy, S.; Read, J. *The Shell Bitumen Handbook*, 6th ed.; ICE Publishing: London, UK, 2015.